Particle number fluctuations and correlations in transfer reactions obtained using the Balian-Veneroni variational principle

Cédric Simenel

Particle number fluctuations and correlations in transfer reactions obtained using the Balian-Vénéroni variational principle

Cédric Simenel[1, 2, *]

[1] *Department of Nuclear Physics, Research School of Physics and Engineering, Australian National University, Canberra, Australian Capital Territory 0200, Australia*
[2] *CEA, Centre de Saclay, IRFU/Service de Physique Nucléaire, F-91191 Gif-sur-Yvette, France.*

(Dated: November 22, 2010)

The Balian-Vénéroni (BV) variational principle, which optimizes the evolution of the state according to the relevant observable in a given variational space, is used at the mean-field level to determine the particle number fluctuations in fragments of many-body systems. For fermions, the numerical evaluation of such fluctuations requires the use of a time-dependent Hartree-Fock (TDHF) code. Proton, neutron and total nucleon number fluctuations in fragments produced in collisions of two ^{40}Ca nuclei are computed for a large range of angular momenta at a center of mass energy $E_{cm} = 128$ MeV, well above the fusion barrier. For deep-inelastic collisions, the fluctuations calculated from the BV variational principle are much larger than standard TDHF results. For the first time, a good reproduction of mass and charge experimental fluctuations is obtained, and the correlations between proton and neutron numbers are determined, within a quantum microscopic approach.

The quantum many-body problem is the root of many theoretical physics fields aiming to describe the structure and dynamics of interacting particles such as electrons in metals, molecules, atomic clusters, Bose-Einstein condensates, or atomic nuclei [1]. However, it can be solved exactly for simple cases only. In most practical applications, mean-field models are considered in a first approximation, and, eventually, serve as a basis for beyond-mean-field approaches [2, 3]. In mean-field theories, the interaction between the particles is replaced by a one-body mean-field potential generated by all the particles. It is, then, assumed that each particle evolves independently in this potential.

For instance, N independent fermions may be described by a Slater determinant $|\phi\rangle = \prod_{i=1}^{N} \hat{a}_i^\dagger |-\rangle$, where $\hat{a}_i^\dagger$ creates a particle in the state $|\varphi_i\rangle$. In such a state, all the information is contained in the one-body density-matrix ρ associated to the operator $\hat{\rho} = \sum_{i=1}^{N} |\varphi_i\rangle\langle\varphi_i|$. The self-consistent mean-field evolution of ρ is given by the time-dependent Hartree-Fock (TDHF) equation [4]

$$i\hbar\frac{\partial\rho}{\partial t} = [h[\rho], \rho]\,, \tag{1}$$

where $h[\rho]$ is the Hartree-Fock (HF) single-particle Hamiltonian with matrix elements $h_{\alpha\beta} = \frac{\delta\langle\phi|\hat{H}|\phi\rangle}{\delta\rho_{\beta\alpha}}$, $\hat{H}$ is the full Hamiltonian, and $\rho_{\alpha\beta} = \langle\varphi_\alpha|\hat{\rho}|\varphi_\beta\rangle = \langle\phi|\hat{a}_\beta^\dagger\hat{a}_\alpha|\phi\rangle$.

Equation 1 is obtained by solving the variational principle where the Dirac action

$$S_D = \int_{t_0}^{t_1} dt\ \langle\phi|\left(i\hbar\frac{\partial}{\partial t} - \hat{H}\right)|\phi\rangle \tag{2}$$

is required to be stationary in the subspace of Slater determinants $|\phi\rangle$ with fixed boundary conditions at times t_0 and t_1. The TDHF approach is usually sufficient to predict the expectation values of one-body observables $\hat{X} = \sum_{i=1}^{N} \hat{q}_X(i)$ but may fail to reproduce their fluctuations and correlations determined from

$$\sigma_{XY} = \sqrt{\langle\hat{X}\hat{Y}\rangle - \langle\hat{X}\rangle\langle\hat{Y}\rangle}, \tag{3}$$

as, e.g., in deep-inelastic heavy-ion collisions [5]. This is an intrinsic limitation of this variational principle combined with the constraint that the state is a single Slater determinant at any time [6]. The knowledge of such fluctuations is, however, crucial to all quantum systems. Thus, their theoretical prediction is an important challenge for quantum many-body models.

The limitation discussed above can be overcome thanks to the Balian and Vénéroni (BV) variational principle based on the action [7–10]

$$S_{BV} = \mathrm{Tr}\hat{D}(t_1)\hat{B}(t_1) - \int_{t_0}^{t_1} dt\ \mathrm{Tr}\left(\hat{B}\frac{\partial\hat{D}}{\partial t} - i\hat{D}[\hat{H}, \hat{B}]\right), \tag{4}$$

where $\hat{B}$ and $\hat{D}$ are the time-dependent trial observable and density matrix of the trial state, respectively, and Tr denotes a trace in the Fock space. They are constrained to obey the boundary conditions $\hat{D}(t_0) = \hat{D}_0$ and $\hat{B}(t_1) = \hat{Q}$, where $\hat{D}_0$ is the initial state and $\hat{Q}$ is the operator we want to evaluate at time t_1. If one chooses independent particle states, $\hat{D} = |\phi\rangle\langle\phi|$, and one-body observables, $\hat{B} = \hat{X}$, for the variational spaces, one recover the TDHF equation (1) [8]. According to this variational approach, TDHF is, then, the best mean-field theory to describe expectation values of one-body observables, but cannot be used, in principle, to determine their fluctuations and correlations which are outside the variational space for $\hat{B}(t)$. To obtain such fluctuations, the variational space has to be increased to $\hat{B} \in \{e^{\gamma\hat{a}^\dagger\hat{a}}\}$ [9, 10]. The observable to be evaluated is $\hat{Q} = \exp(-\lambda_1\hat{X} - \lambda_2\hat{Y})$. Indeed, fluctuations and correlations can be recovered

for small λ_1 and λ_2 using $\ln\langle\exp(-\lambda_1\hat{X} - \lambda_2\hat{Y})\rangle \simeq -\lambda_1\langle\hat{X}\rangle - \lambda_2\langle\hat{Y}\rangle + \frac{\lambda_1^2}{2}\sigma_{XX} + \frac{\lambda_2^2}{2}\sigma_{YY} + \lambda_1\lambda_2\sigma_{XY}$. Keeping the approximation $\hat{D} = |\phi\rangle\langle\phi|$, this leads to [10]

$$\sigma^2_{XY}(t_1) = \lim_{\epsilon\to 0} \frac{\mathrm{tr}\left[\rho(t_0) - \rho_X(t_0,\epsilon)\right]\left[\rho(t_0) - \rho_Y(t_0,\epsilon)\right]}{2\epsilon^2}, \tag{5}$$

where tr denotes a trace in the single-particle space. The one-body density matrices $\rho_X(t,\epsilon)$ obey the TDHF equation (1) with the boundary condition

$$\rho_X(t_1,\epsilon) = \exp(i\epsilon q_X)\rho(t_1)\exp(-i\epsilon q_X), \tag{6}$$

where q_X is the matrix representing the single particle operator $\hat{q}_X$. In Eq. (6), $\rho(t)$ is the solution of the TDHF equation (1). The initial condition $\rho(t_0)$ is derived from the initial density matrix $\hat{D}_0 = |\phi_0\rangle\langle\phi_0|$ by $\rho_{\alpha\beta}(t_0) = \mathrm{Tr}\hat{a}^\dagger_\beta\hat{a}_\alpha\hat{D}_0 = \langle\phi_0|\hat{a}^\dagger_\beta\hat{a}_\alpha|\phi_0\rangle$.

The optimum mean-field prediction of σ_{XY} in Eq. (5) differs from the "standard" TDHF expression which is evaluated from Eq. (3) using $\rho(t_1)$:

$$\sigma^2_{XY}(t_1) = \mathrm{tr}\{q_Y\rho(t_1)q_X\left[I - \rho(t_1)\right]\}, \tag{7}$$

where I is the identity matrix. Although both Eqs. (5) and (7) are associated to mean-field approximations, the first one is more general as it is derived using a larger variational space for the observable evolution. In the next, BV and TDHF fluctuations or correlations refer to Eq. (5) and (7), respectively. Before to discuss the present calculations, let us first summarize previous applications of the BV variational principle.

Earlier works have focused on particle number fluctuations in nuclear collective vibrations [11] and in heavy-ion collisions [12, 13]. Marston *et al.* [13] have also investigated the fluctuations in momentum and kinetic energy of the fragments. The technique used in these works is similar to the one employed here. However, the use of simple effective interactions and geometry restrictions in the TDHF codes were strong limitations which prevent realistic predictions. Thus, their results should be considered only as qualitative. In these works, the BV fluctuations are always larger than their TDHF counterparts. This is encouraging and constitute a strong motivation for realistic calculations with the BV variational principle to compute fluctuations of one-body observables. Modern three-dimensional TDHF codes [14–17] with full Skyrme energy-density-functional (EDF) [18] including spin-orbit interaction can now be used for realistic applications of the BV variational principle. Recent calculations using such a code have been made to determine particle fluctuations in the daughter nucleus produced in giant dipole resonance decay [19] and in nuclear collisions [20].

In this work, the predictive power of the BV variational principle is illustrated in realistic calculations of heavy-ion collisions in comparison with experimental data. The fluctuations σ_{NN}, σ_{ZZ}, and σ_{AA}, where N and Z are the neutron and proton numbers, respectively, and $A = N + Z$, are computed in fragments resulting both from deep-inelastic and quasi-elastic collisions. The correlations σ_{NZ} are determined for the first time within a quantum microscopic approach, thanks to the BV variational principle.

The TDHF3D code is used to compute σ_{XY} from the BV variational principle with the SLy4d parameterization of the EDF [14]. The TDHF equation (1) is solved iteratively in time, with a time step $\Delta t = 1.5\times10^{-24}$ s, in the center of mass frame. A smaller time step, $\Delta t = 1.0\times10^{-24}$ s, has also been used to confirm the convergence of the BV fluctuations. The single-particle wave-functions are evolved on a Cartesian grid of $56\times56\times28/2$ points with a plane of symmetry (the collision plane) and a mesh-size $\Delta x = 0.8$ fm. The initial distance between collision partners is 22.4 fm. Refs. [2, 21] give more details of the TDHF calculations.

To evaluate BV fluctuations from Eq. (5), the first step is to perform a TDHF evolution forward in time from t_0 to t_1. To account for the transformation of Eq. (6), at time t_1, the occupied single particle wave functions are boosted according to

$$|\varphi_{X_j}(t_1,\epsilon)\rangle = \exp(i\epsilon q_{X_j}\Theta(\hat{\mathbf{r}}))|\varphi_j(t_1)\rangle, \tag{8}$$

where X stands for N, Z, or A. If the occupied single particle wave-function φ_j refers to a proton (resp. a neutron), we have $q_{N_j} = 0$ and $q_{Z_j} = 1$ (resp. $q_{N_j} = 1$ and $q_{Z_j} = 0$), while $q_{A_j} = 1$ for protons and neutrons. The function $\Theta(\mathbf{r})$ is equal to 1 for the fragment on which the fluctuations are calculated, and $\Theta(\mathbf{r}) = 0$ for the other one. Arbitrarily, σ_{XY} are measured on the fragment which has its center of mass in the $x+y>0$ plane. The time t_1 is determined, for each collision, by the time at which at least one fragment center of mass reaches 11.2 fm from one edge of the box. This prevents spurious distortion of the wave functions due to the hard boundary conditions. It also ensures a minimum separation distance of 22.4 fm for symmetric collisions. This value is large enough to ensure a convergence of σ_{XY} with t_1 as the fragments interact only via Coulomb repulsion at this distance [12, 13].

The second step is to compute a backward evolution from t_1 to t_0 of each set of single particle wave functions $\varphi_{X_i}(t,\epsilon)$. Several values of $10^{-3} \le \epsilon \le 10^{-2}$ are considered to determine the limit in Eq (5). Following Refs. [12, 20], the initial density matrix $\rho(t_0)$ in Eq. (5) is replaced by a backward evolved density matrix $\rho_I(t_0,\epsilon = 0)$, i.e., without the transformation in Eq. (6), to minimize numerical inaccuracies. Note that the latter are easily controllable and this procedure is not necessary with a smaller time step Δt. The trace in Eq. (5) is then evaluated with $\mathrm{tr}\left[\rho_I(t_0,0) - \rho_X(t_0,\epsilon)\right]\left[\rho_I(t_0,0) - \rho_Y(t_0,\epsilon)\right] = \eta_{II} +$

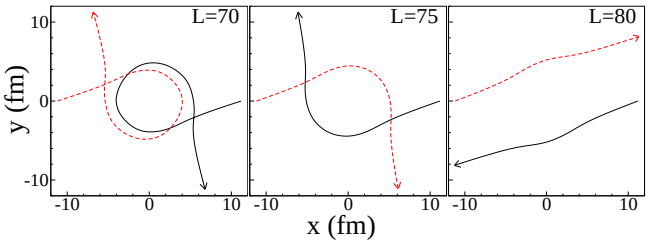

FIG. 1: Evolution of the fragment centers of mass for ^{40}Ca+^{40}Ca at $E_{cm} = 128$ MeV, for different angular momenta L in unit of $\hbar$.

$\eta_{XY} - \eta_{IX} - \eta_{IY}$, where $\eta_{XX'} = \sum_{ij} \left| \langle \varphi_{X_i}(t_0) | \varphi_{X'_j}(t_0) \rangle \right|^2$ and the sums run over occupied states. The quadratic evolution of the trace with ϵ is used as a convergence check [13], as well as the property $\eta_{II} = A_t$, where A_t is the total number of nucleons.

Let us investigate the collision of two ^{40}Ca nuclei at a center of mass energy $E_{cm} = 128$ MeV. The calculations have been performed in steps of $5\hbar$ starting with orbital angular momentum $L = 65$, for which a capture reaction occurs (defined as no re-separation of the fragments after a calculation until 135×10^{-22} s), to $L = 100$, corresponding to a quasi-elastic reaction. Figure 1 shows the trajectories of the fragment centers of mass for $L = 70, 75$, and 80, corresponding to the most violent collisions leading to two fragments in the exit channel which have been investigated in this work. We see that a wide range of scattering angles may occur at angular momenta around $L = 70$, which is a known feature of deep-inelastic collisions. Experimentally, mass and charge fluctuations for deep-inelastic collisions are then determined at large scattering angles [22, 23].

The TDHF fluctuations [Eq. (7)] have been determined from the probability distributions of A, Z and N in the fragments at time t_1 using a particle number projection technique [21]. The resulting fluctuations σ_{AA} and σ_{ZZ} are shown in Fig. 2 by dashed lines. The fluctuations obtained from the BV variational principle using Eq. (5) are shown by solid lines. They are much more important than the TDHF predictions for $L \leq 80$. However, at large L (quasi-elastic reactions), the BV and TDHF mass fluctuations are similar. The neutron fluctuations σ_{NN} are not shown for clarity as they are very similar to the proton ones.

Charge fluctuations have been measured experimentally for this system by Roynette *et al* [22]. They obtained a plateau at $\sigma_{ZZ}^{exp} \simeq 5$ for scattering angles $\theta_{cm} \geq 50$ deg, associated to deep-inelastic collisions. The calculations show that these scattering angles are obtained for angular momenta in the range 65-75 (see Fig. 1). The BV fluctuation is $\sigma_{ZZ} \simeq 4.3$ at $L \simeq 70$ (see Fig. 2), in good agreement with the experimental value, while TDHF underestimates σ_{ZZ}^{exp} by a factor of

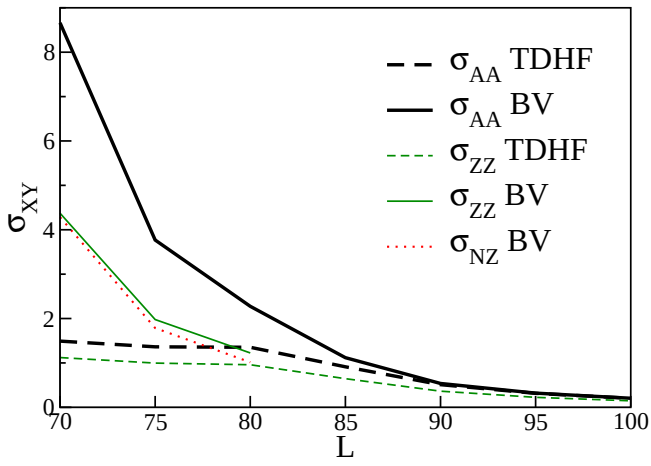

FIG. 2: TDHF (dashed lines) and BV (solid lines) fluctuations of A (thick black) and Z (thin green) for ^{40}Ca+^{40}Ca at $E_{cm} = 128$ MeV as a function of angular momentum L in units of $\hbar$. BV correlations between N and Z are also shown (dotted line). BV predictions of σ_{ZZ} and σ_{NZ} have been computed for $L \leq 80$ only.

~ 5. Note that the theoretical predictions are made for the primary (excited) fragment. As the fragments cool down by nucleon emission, their mass and charge fluctuations might increase [19]. However, this increase from evaporation process should remain a small correction [5]. The fragment mass distribution has also been measured for the ^{40}Ca+^{40}Ca system by Evans *et al.*, but at lower energies, $E_{cm} = 98.5$ and 115.5 MeV [23]. Their data are consistent with $\sigma_{AA} \simeq 11$ for the primary fragment mass distribution. Considering the uncertainties in the reconstruction of the primary fragment masses, their result is in reasonable agreement with the BV fluctuations $\sigma_{AA} \simeq 8.7$ at $L = 70$ (see Fig. 2).

At this point, it is worth mentioning that these calculations show the first reproduction of experimental mass and charge fluctuations from a fully quantum microscopic formalism with no adjustable parameter. Indeed, earlier calculations of σ_{AA} [13] were, in fact, compared to σ_{ZZ} experimental values [24] (see discussion in Ref. [20]), and, therefore, strongly underestimated the experimental data. In addition, they neglected the spin-orbit interaction which is known to generate important dissipation in nuclear collisions [25]. In fact, repeating the calculations of [13] for ^{40}Ca+^{40}Ca at $L = 30$ and $E_{cm} = 139$ MeV, with a full Skyrme functional, Broomfield obtained a capture reaction instead of a deep-inelastic collision [20].

In addition to fluctuations, the BV correlations σ_{NZ} between the proton and neutron numbers in the fragments have been computed from Eq. (5) (dotted line in Fig. 2). These finite values of σ_{NZ} are at variance with the TDHF correlations which are strictly zero. This was checked numerically using $\sigma_{NZ}^2 = (\sigma_{AA}^2 - \sigma_{ZZ}^2 - \sigma_{NN}^2)/2$. However, this is not an intrinsic limitation of the TDHF

formalism, but a consequence of the constraint that the single particle states have a pure isospin, as in most TDHF applications in nuclear physics. In fact, the probability $P(N,Z)$ to have a fragment with Z and N, in standard TDHF calculations, is the product of the probabilities $P(Z)P(N)$ to have Z and N, independently [21]. For instance, in the symmetric collisions studied here, the TDHF probability to have the $N = Z$ ^{32}S nucleus is the same than for the neutron rich ^{40}S. The production of the latter should, however, be hindered by the symmetry energy which is known to induce a fast charge equilibration in the fragments [26]. The BV prediction of σ_{NZ} are of the same order of magnitude as σ_{ZZ} and σ_{NN} in deep-inelastic collisions (see Fig. 2). The predictions of such correlations are another attractive feature of the BV variational principle and may be compared with experimental data where both mass and charge of each fragment are measured.

Quantum microscopic calculations of particle number fluctuations in fragments produced in heavy-ion collisions have been determined with the Balian-Véneroni variational principle in a mean-field approximation with a three-dimensional TDHF code and a full Skyrme functional. The resulting fluctuations are of the same order as the "standard" TDHF ones in quasi-elastic reactions. In deep-inelastic collisions, however, they are much larger than the TDHF ones. Charge and mass fluctuations in deep-inelastic collisions are in good agreement with experimental data. The correlations between proton and neutron numbers in the fragment distributions have been determined for the first time with a microscopic quantum approach. Applications to multi-nucleon transfer in actinide collisions could be used to predict probabilities for super-heavy element production [27, 28]. The role of pairing correlations on fluctuations should be investigated using independent quasi-particle states. This could be done thanks to recent developments of time-dependent Hartree-Fock-Bogoliubov codes [29–31]. Stochastic-mean-field methods might also be applied to investigate the role of initial beyond-mean-field correlations on fluctuations in deep-inelastic collisions [32].

M. Dasgupta, D. J. Hinde, and D. Lacroix are thanked for discussions and a careful reading of the paper. The calculations have been performed on the NCI National Facility in Canberra, Australia, which is supported by the Australian Commonwealth Government. The author acknowledges the support of ARC Discovery grant DP 0879679.

* cedric.simenel@cea.fr

[1] J. W. Negele and H. Orland, *Quantum Many-particle Systems (Advanced Books Classics)* (Westview Press, 1998), ISBN 0738200522.
[2] C. Simenel, D. Lacroix, and B. Avez, *Quantum Many-Body Dynamics: Applications to Nuclear Reactions* (VDM Verlad, 2010).
[3] D. Lacroix, S. Ayik, and P. Chomaz, Prog. Part. Nucl. Phys. **52**, 497 (2004).
[4] P. A. M. Dirac, Proc. Camb. Phil. Soc. **26**, 376 (1930).
[5] S. E. Koonin, K. T. R. Davies, V. Maruhn-Rezwani, H. Feldmeier, S. J. Krieger, and J. W. Negele, Phys. Rev. C **15**, 1359 (1977).
[6] C. H. Dasso, T. Døssing, and H. C. Pauli, Z. Phys. A **289**, 395 (1979).
[7] R. Balian and M. Véneroni, Phys. Rev. Lett. **47**, 1353 (1981).
[8] R. Balian and M. Véneroni, Ann. Phys. **164**, 334 (1985).
[9] R. Balian and M. Véneroni, Phys. Lett. B **136**, 301 (1984).
[10] R. Balian and M. Véneroni, Annals of Physics **216**, 351 (1992).
[11] T. Troudet and D. Vautherin, Phys. Rev. C **31**, 278 (1985).
[12] P. Bonche and H. Flocard, Nucl. Phys. A **437**, 189 (1985).
[13] J. B. Marston and S. E. Koonin, Phys. Rev. Lett. **54**, 1139 (1985).
[14] K.-H. Kim, T. Otsuka, and P. Bonche, J. Phys. G **23**, 1267 (1997).
[15] T. Nakatsukasa and K. Yabana, Phys. Rev. C **71**, 024301 (2005).
[16] J. A. Maruhn, P. G. Reinhard, P. D. Stevenson, J. R. Stone, and M. R. Strayer, Phys. Rev. C **71**, 064328 (2005).
[17] A. S. Umar and V. E. Oberacker, Phys. Rev. C **71**, 034314 (2005).
[18] T. Skyrme, Phil. Mag. **1**, 1043 (1956).
[19] J. M. A. Broomfield and P. D. Stevenson, J. Phys. G **35**, 095102 (2008).
[20] J. M. A. Broomfield, Ph.D. thesis, University of Surrey (2009).
[21] C. Simenel, Phys. Rev. Lett. **105**, 192701 (2010).
[22] J. C. Roynette, H. Doubre, N. Frascaria, J. C. Jacmart, N. Poffe, and M. Riou, Phys. Lett. B **67**, 395 (1977).
[23] P. Evans, A. Smith, C. Pass, L. Stuttg, B. Back, R. Betts, B. Dichter, D. Henderson, S. Sanders, F. Videbaek, et al., Nucl. Phys. A **526**, 365 (1991).
[24] P. Colombani, N. Frascaria, J. C. Jacmart, M. Riou, C. Stphan, H. Doubre, N. Poff, and J. C. Roynette, Phys. Lett. B **55**, 45 (1975).
[25] A. S. Umar, M. R. Strayer, and P. G. Reinhard, Phys. Rev. Lett. **56**, 2793 (1986).
[26] Y. Iwata, T. Otsuka, J. A. Maruhn, and N. Itagaki, Phys. Rev. Lett. **104**, 252501 (2010).
[27] C. Golabek and C. Simenel, Phys. Rev. Lett. **103**, 042701 (2009).
[28] D. J. Kedziora and C. Simenel, Phys. Rev. C **81**, 044613 (2010).
[29] B. Avez, C. Simenel, and P. Chomaz, Phys. Rev. C **78**, 044318 (2008).
[30] S. Ebata, T. Nakatsukasa, T. Inakura, K. Yoshida, Y. Hashimoto, and K. Yabana, Phys. Rev. C **82**, 034306 (2010).
[31] K. Washiyama and D. Lacroix, private communication.
[32] K. Washiyama, S. Ayik, and D. Lacroix, Phys. Rev. C **80**, 031602 (2009).